Temperature dependence of Raman shifts in layered $ReSe_2$ and $SnSe_2$ semiconductor nanosheets

A. Taube,[a),b)] A. Łapińska,[b)] J. Judek, and M. Zdrojek[c)]
Faculty of Physics, Warsaw University of Technology, Koszykowa 75, 00-662 Warsaw, Poland

(Received 21 April 2015; accepted 29 June 2015; published online 8 July 2015)

Transition metal dichalcogenides (TMDCs) are attractive for variety of nanoscale electronics and optoelectronics devices due to their unique properties. Despite growing progress in the research field of TMDCs, many of their properties are still unknown. In this letter, we report measurements of Raman spectra of rhenium diselenide ($ReSe_2$) and tin diselenide ($SnSe_2$) layered semiconductor nanosheets as a function of temperature (70–400 K). We analyze the temperature dependence of the positions of eight $ReSe_2$ modes and $SnSe_2$ A_{1g} mode. All observed Raman mode shifts exhibit nonlinear temperature dependence at low temperatures which is explained by optical phonon decay process into two or three acoustics phonons. The first order temperature coefficients (χ), determined for high temperatures, of rhenium diselenide Raman modes are in the range between -0.0033 and $-0.0118\,cm^{-1}/K$, whereas χ of tin diselenide A_{1g} mode was $-0.0129\,cm^{-1}/K$. Our findings are useful for further analysis of phonon and thermal properties of these dichalcogenide layered semiconductors. © *2015 AIP Publishing LLC*. [http://dx.doi.org/10.1063/1.4926508]

Layered transition metal dichalcogenides (TMDCs) have attracted considerable attention of researchers because of their unique electronic, optical, and mechanical properties.[1] TMDCs are a family of compounds with a general chemical formula MX_2, wherein M is a metal atom, and X is atom of sulfur (*S*), selenium (*Se*), or tellurium (*Te*).[2] The most intensively studied TMDCs are semiconductors such as molybdenum disulfide (MoS_2), tungsten disulfide (WS_2), and tungsten diselenide (WSe_2). On the basis of these compounds, a variety of electronic, optoelectronic, and thermoelectric[3] devices, like transistors,[4] digital circuits,[5] photodetectors,[6] and light emitting diodes,[7] were demonstrated.

Among newly discovered TMDCs, rhenium compounds, i.e., rhenium disulfide (ReS_2) and rhenium diselenide ($ReSe_2$) are characterized by unexpected and very interesting properties.[8–11] First of all, unlike most dichalcogenides e.g., MoS_2, $SnSe_2$, or WSe_2, which possess hexagonal like phase, $ReSe_2$, and ReS_2 crystallize in distorted 1-T phase (triclinic) with a large unit cell having only a center of inversion (Figs. 1(a) and 1(b)). Moreover, the four Re atoms from unit cell are arranged in-plane into "lozenge" shape which forms the "Re chain" along b-axis.

This leads to exceptional anisotropic electronic[11] and optical properties.[12,13] The weak interlayer interactions lead to the situation that bulk material behaves like a monolayer. For ReS_2, it was shown that the direct band gap, Raman spectra, and photoluminescence spectra vary slightly with increasing the number of layers,[14] which is in contrast to other TMDCs where crossover from indirect to direct band gap occurs with decreasing the number of layers from bulk to monolayer.[15] On the other hand, other hexagonal dichalcogenides, like tin diselenide ($SnSe_2$), were not extensively studied. There are few reports on the electronic and optoelectronic devices based on $ReSe_2$[8,9] and $SnSe_2$[16] that show the applicability of these compounds. However, many properties of TMDCs like phonon and thermal properties of compounds from this family are still poorly understood. Prior works on the Raman spectroscopy of $ReSe_2$ and $SnSe_2$ have been focused on polarization study[12] or concerned the bulk crystals.[17]

In this work, we present temperature dependent Raman shifts in rhenium diselenide and tin diselenide nanosheets. We show that temperature dependence of Raman modes exhibits nonlinear behavior for low temperatures which was explained by optical phonon decay into two and three acoustic phonons. For high temperatures, position of Raman modes tends to a linear dependence and first order temperature coefficients (χ) were extracted.

Figures 1(a), 1(b), 1(e), and 1(f) show crystalline structures of investigated triclinic $ReSe_2$ and hexagonal $SnSe_2$ along c- and a-axes. On the top-view of $ReSe_2$ "Re chain" was marked. The $ReSe_2$ and $SnSe_2$ thin flakes were fabricated on SiO_2 (275 nm)/Si substrate by conventional mechanical exfoliation technique[18,19] from bulk single crystals (2dsemiconductors). Optical microscopy and atomic force microscopy (AFM) images of investigated nanosheets are depicted in Figs. 1(c) and 1(g). The thickness measured by AFM was 30 nm and 107 nm for $ReSe_2$ and $SnSe_2$ flakes, respectively. We note that the temperature dependent Raman measurements were repeated on several samples with different thickness and the trend in results was fairly consistent. The unpolarized Raman spectra were collected using a 50× objective and a He-Ne laser 632.8 nm (1.96 eV) excitation wavelength in backscattering geometry. The laser power, calibrated on the sample, was relatively low (0.2 mW) to avoid laser heating. The resolution of peak position was $\sim 0.5\,cm^{-1}$ in one spectral window. Temperature-dependent

[a)]Also with Institute of Electron Technology, Warsaw, Poland and Institute of Microelectronics and Optoelectronics, Warsaw University of Technology, Warsaw, Poland.
[b)]A. Taube and A. Łapińska contributed equally to this work.
[c)]Author to whom correspondence should be addressed. Electronic mail: zdrojek@if.pw.edu.pl. Tel./Fax: +48 22 234 7170.

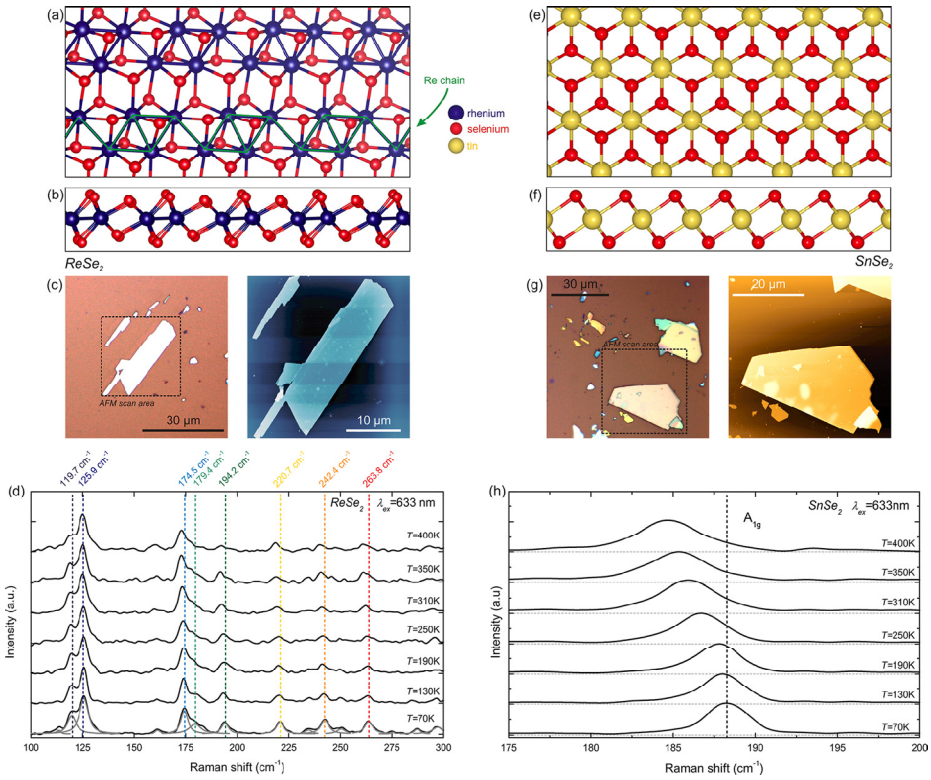

FIG. 1. Crystal structure of rhenium diselenide ((a) along c-axis and (b) along a-axis) and tin diselenide ((e) along c-axis and (f) along a-axis). Optical microscope and AFM image of (c) $ReSe_2$ and (g) $SnSe_2$. Raman spectra of the (d) $ReSe_2$ and (h) $SnSe_2$ measured in temperature range between 70 K and 400 K.

Raman scattering studies were carried out under vacuum by heating and cooling the sample in a microscope cryostat with temperature controlled between 70 K and 400 K (temperature stability was about 0.1 K). For each temperature point, the measurements were performed several times in order to minimize the statistical error. The Lorenzian functions were fitted to the experimental data using Levenberg-Marquad algorithm.

The group theory analysis predicts 36 modes as $ReSe_2$ ($P\bar{1}$ space group) has 12 atoms per unit cell. The $ReSe_2$ has

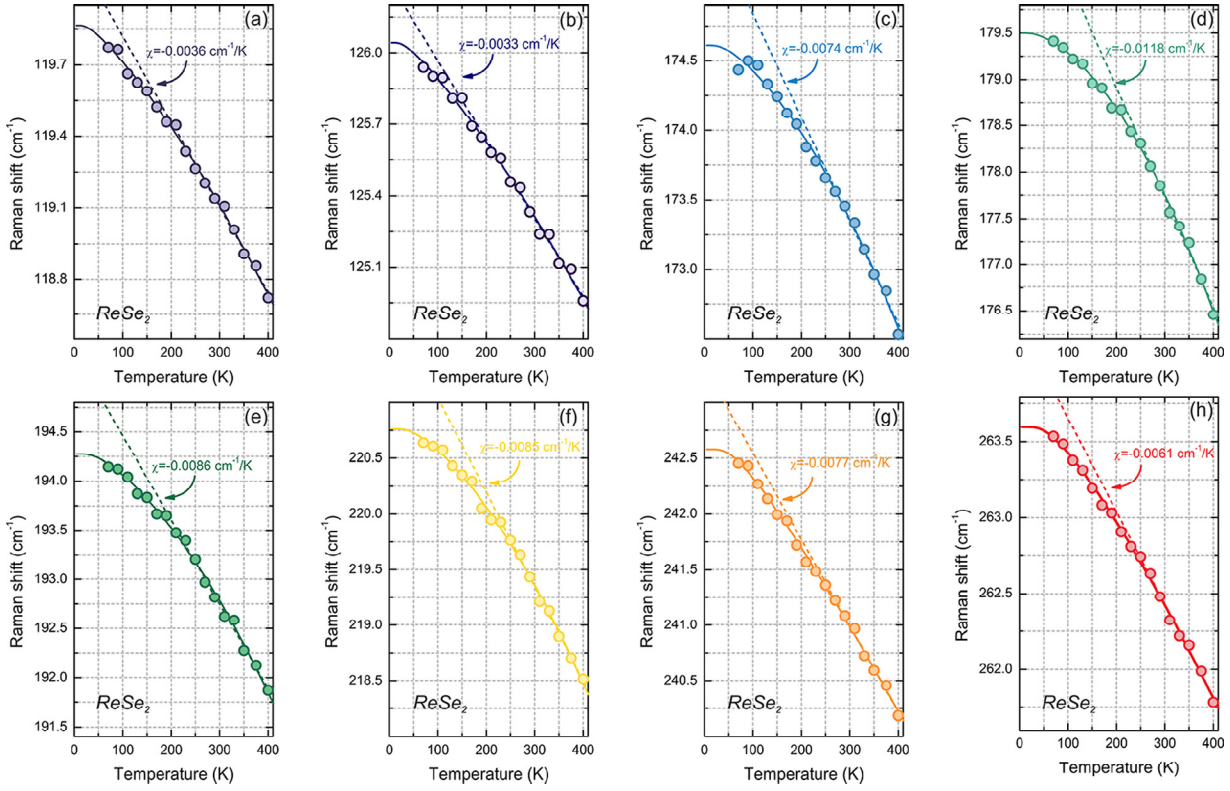

FIG. 2. Temperature dependence of (a) 119.7 cm^{-1}, (b) 125.9 cm^{-1}, (c) 174.5 cm^{-1}, (d) 179.4 cm^{-1}, (e) 194.2 cm^{-1}, (f) 220.7 cm^{-1}, (g) 242.4 cm^{-1}, and (h) 263.8 cm^{-1} rhenium diselenide Raman modes.

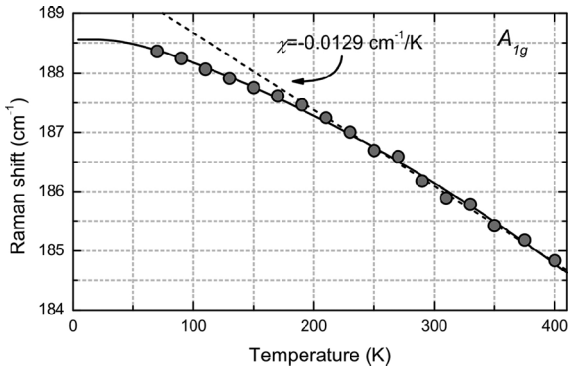

FIG. 3. Temperature dependence of tin diselenide A_{1g} mode position.

18 Raman active A_g modes, 15 infrared active A_u modes, and 3 zero-frequency A_u modes.[12] For $SnSe_2$ ($P\bar{3}ml$ space group) theory predicts one A_{1g} and E_g mode and 3 infrared active A_{2u} and E_u modes.[20] In Figures 1(d) and 1(h), the measured Raman spectra are shown for selected temperatures between 70 K and 400 K. For $ReSe_2$, in spectra measured at 70 K, fifteen out of eighteen Raman active modes were observed with the following positions: 113.2, 119.7, 125.9, 161.4, 174.4, 179.4, 194.2, 220.6, 234.6, 242.4, 250.4, 263.8, 274.8, 287.3, and 297.4 cm^{-1}. For $SnSe_2$, two main Raman modes A_{1g} and E_g were observed at 188.3 and 115.5 cm^{-1}, respectively. All $ReSe_2$ and $SnSe_2$ Raman modes are downshifted with increasing temperatures and show clearly nonlinear behavior at low temperatures. For further detailed analysis, we have selected the eight most intensive $ReSe_2$ modes (119.7, 125.9, 174.5, 179.4, 194.2, 220.7, 242.4, and 263.8 cm^{-1}). Note that for the convenience, the Raman modes of $ReSe_2$ are labelled in the manuscript by their position at 70 K. The $SnSe_2$ E_g mode was weak and hard to resolve (data not shown) and consequently was excluded from further analysis. The detailed, calculated position of selected $ReSe_2$ and $SnSe_2$ Raman modes are shown in Figures 2 and 3.

In general, several factors are responsible for temperature dependence of Raman shift like electron-phonon, anharmonic phonon-phonon interactions, and thermal expansion. In our case, to describe phonon softening due to temperature increase, we used approach developed by Balkanski *et al.*,[21] where temperature dependence of Raman modes arises from phenomenon of the optical phonon decay into two (three phonon process) or three (four phonon process) acoustic phonons with equal energies stemming from lattice potential cubic and quartic anharmonicity. Balkanski *et al.* proposed following formula to describe temperature dependence of Raman modes:[21]

$$\omega(T) = \omega_0 + A\left[1 + \frac{2}{e^x - 1}\right] + B\left[1 + \frac{3}{e^y - 1} + \frac{3}{(e^y - 1)^2}\right], \quad (1)$$

where $x = \hbar\omega_0/2k_bT$, $y = \hbar\omega_0/3k_bT$, ω_0 is phonon frequency at $T = 0$ K, $\hbar$ is Planck's constant divided by 2π, k_b is Boltzmann constant, and A and B are anharmonic constants. This approach was used in order to explain temperature dependence of position of Raman modes of silicon,[21] gallium arsenide,[22] and recently supported molybdenum disulfide monolayers[23] and carbon nanotube thin films.[24] For temperatures above 210 K, the positions of Raman modes tend to linear dependence and can be described by first order temperature coefficient (χ) according to Eq. (2)

$$\omega(T) = \omega_0 + \chi T, \quad (2)$$

where ω_0 is the phonon frequency for temperature extrapolated to 0 K and χ is the first-order temperature coefficient. This approach is commonly used for describing temperature-dependence of Raman shifts of various nanomaterials.[25–29] The calculated ω_0, A, and B anharmonic constants and χ values are presented in Table I for $ReSe_2$ and Table II for $SnSe_2$. The fits to Eqs. (1) and (2) are also depicted in Figures 2 and 3. For all analyzed $ReSe_2$ and $SnSe_2$ Raman modes, anharmonic constant A is several times larger than B constant. This suggests that the probability of the three phonon process is greater than the probability of four phonon process.[21]

As it can be noticed, there is a large difference between the temperature induced downshifts for different modes. The most intensive peaks, at 119.7 and 125.9 cm^{-1}, are shifted by about 1.05 and 0.98 cm^{-1}, respectively, for temperature increase from 70 K to 400 K. The calculated χ values were about −0.0033 and −0.0036 cm^{-1}/K which are several times smaller than χ value for other TMDCs and nanomaterials like MoS_2 ($\chi = -0.0178$ cm^{-1}/K for A_{1g} mode[23]), graphene ($\chi = -0.016$ cm^{-1}/K for G mode[30]), or phosphorene ($\chi = -0.023$ cm^{-1}/K for A_g and A_g^2 modes[31]). The largest temperature coefficient χ was observed for 179.4 cm^{-1} mode which was −0.0118 cm^{-1}/K, and the mode position was red-shifted by about 2.95 cm^{-1} as temperature changes from 70 K to 400 K.

The small first order temperature coefficients of rhenium diselenide Raman modes may arise from weak interactions between the individual layers as it is in the case of $ReSe_2$; however, particular mechanism has to be fully determined. It is known that first order temperature coefficient of layered materials is related to the van der Waals interactions between individual layers (for details, see Ref. 32). Moreover, it was

TABLE I. Calculated parameters from fit of Eqs. (1) and (2) to temperature dependence of the positions of $ReSe_2$ Raman modes.

ω (70 K)	119.7	125.9	174.5	179.4	194.2	220.7	242.4	263.8
ω_0 (cm^{-1})	119.9	126.1	174.8	179.6	194.5	221.0	243.2	264.1
A (cm^{-1})	−0.088	−0.098	−0.133	−0.078	−0.19	−0.215	−0.57	−0.40
B (cm^{-1})	−0.0027	−0.002	−0.019	−0.04	−0.03	−0.03	−0.008	−0.015
χ (cm^{-1}/K)[a]	−0.0036	−0.0033	−0.0074	−0.0118	−0.0086	−0.0085	−0.0078	−0.0061

[a]Calculated for 210–400 K temperature range.

TABLE II. Calculated parameters from fit of Eqs. (1) and (2) to temperature dependence of the position of $SnSe_2$ A_{1g} Raman mode.

A_{1g}			
ω_0 (cm^{-1})	A (cm^{-1})	B (cm^{-1})	χ (cm^{-1}/K)[a]
188.84	−0.41	−0.03	−0.0129

[a]Calculated for 210–400 K temperature range.

shown that the first order temperature coefficient is related to the interaction between the silicon carbide substrate and the epitaxial graphene as χ was larger for pinned layers prepared by sublimation method compared to unpinned CVD graphene.[33]

The position of $SnSe_2$ A_{1g} mode decreases by about 3.5 cm^{-1} when temperature increases from 70 K to 400 K. The temperature dependence of this mode is more sensitive to a temperature change than in case of any of $ReSe_2$ modes. The determined first order temperature coefficient χ of A_{1g} was −0.0129 cm^{-1}/K and was comparable to the values for other layered nanomaterials.

The knowledge about particular temperature coefficients for different modes is important in thermal metrology based on the Raman spectroscopy, which can be used, for example, for determination of thermal properties like thermal conductivity[34–36] or for *in-situ* monitoring of local temperature of operating device.[37,38] As Raman mode position is more sensitive to temperature change, the smaller is the error of determination of the temperature rise upon the laser or electrical power heating due to finite resolution of spectrometer and variability of peak position.

In conclusion, we have investigated in detail the temperature dependence of Raman shifts in layered rhenium diselenide and tin diselenide semiconductors nanosheets in temperature range between 70 K and 400 K. We analyze position of the 8 most intensive $ReSe_2$ modes of A_g symmetry and $SnSe_2$ A_{1g} mode. We noticed nonlinear behavior of Raman shifts in low temperatures. The results were explained by phenomenon of optical phonon decay into two and three acoustic phonons. We showed that the temperature dependence of Raman shifts of $ReSe_2$ modes was relatively weak. Among $ReSe_2$ modes, the most sensitive to the temperature was 179.4 cm^{-1} mode for which χ was −0.0118 cm^{-1}/K. The first order temperature coefficient for $SnSe_2$ A_{1g} was −0.0129 cm^{-1}/K. The obtained results can be used for further analysis of phonon and thermal properties of those materials, which are still unknown and are to be understood in order to be applied in nanoscale devices.

The work was supported by the Polish Ministry of Science and Higher Education within the Diamond Grant Programme (0025/DIA/2013/42).

[1]Q. H. Wang, K. Kalantar-Zadeh, A. Kis, J. N. Coleman, and M. S. Strano, Nat. Nanotechnol. **7**, 699 (2012).
[2]M. Chhowalla, H. S. Shin, G. Eda, L.-J. Li, K. P. Loh, and H. Zhang, Nat. Chem. **5**, 263 (2013).
[3]J. Wu, H. Schmidt, K. K. Amara, X. Xu, G. Eda, and B. Özyilmaz, Nano Lett. **14**, 2730 (2014).
[4]S. Das, H.-Y. Chen, A. V. Penumatcha, and J. Appenzeller, Nano Lett. **13**, 100 (2013).
[5]H. Wang, L. Yu, Y.-H. Lee, Y. Shi, A. Hsu, M. L. Chin, L.-J. Li, M. Dubey, J. Kong, and T. Palacios, Nano Lett. **12**, 4674 (2012).
[6]O. Lopez-Sanchez, D. Lembke, M. Kayci, A. Radenovic, and A. Kis, Nat. Nanotechnol. **8**, 497 (2013).
[7]A. Pospischil, M. M. Furchi, and T. Mueller, Nat. Nanotechnol. **9**, 257 (2014).
[8]S. Yang, S. Tongay, Q. Yue, Y. Li, B. Li, and F. Lu, Sci. Rep. **4**, 5442 (2014).
[9]S. Yang, S. Tongay, Y. Li, Q. Yue, J.-B. Xia, S.-S. Li, J. Li, and S.-H. Wei, Nanoscale **6**, 7226 (2014).
[10]Y. Feng, W. Zhou, Y. Wang, J. Zhou, E. Liu, Y. Fu, Z. Ni, X. Wu, H. Yuan, F. Miao, B. Wang, X. Wan, and D. Xing, e-print arXiv:1502.02835v1.
[11]E. Liu, Y. Fu, Y. Wang, Y. Feng, H. Liu, X. Wan, W. Zhou, B. Wang, L. Shao, C.-H. Ho, Y.-S. Huang, Z. Cao, L. Wang, A. Li, J. Zeng, F. Song, X. Wang, Y. Shi, H. Yuan, H. Y. Hwang, Y. Cui, F. Miao, and D. Xing, Nat. Commun. **6**, 6991 (2015).
[12]D. Wolverson, S. Crampin, A. S. Kazemi, A. Ilie, and S. J. Bending, ACS Nano **8**, 11154–11164 (2014).
[13]C. H. Ho and C. E. Huang, J. Alloys Compd. **383**, 74 (2004).
[14]S. Tongay, H. Sahin, C. Ko, A. Luce, W. Fan, K. Liu, J. Zhou, Y.-S. Huang, C.-H. Ho, J. Yan, D. F. Ogletree, S. Aloni, J. Ji, S. Li, J. Li, F. M. Peeters, and J. Wu, Nat. Commun. **5**, 3252 (2014).
[15]A. Splendiani, L. Sun, Y. Zhang, T. Li, J. Kim, C.-Y. Chim, G. Galli, and F. Wang, Nano Lett. **10**, 1271 (2010).
[16]Y. Su, M. A. Ebrish, E. J. Olson, and S. J. Koester, Appl. Phys. Lett. **103**, 263104 (2013).
[17]S. V. Bhatt, M. P. Deshpande, V. Sathe, and S. H. Chaki, Solid State Commun. **201**, 54 (2015).
[18]K. S. Novoselov, D. Jiang, F. Schedin, T. J. Booth, V. V. Khotkevich, S. V. Morozov, and A. K. Geim, Proc. Natl. Acad. Sci. U. S. A. **102**, 10451 (2005).
[19]K. S. Novoselov, A. K. Geim, S. V. Morozov, D. Jiang, Y. Zhang, S. V. Dubonos, I. V. Grigorieva, and A. A. Frisov, Science **306**, 666 (2004).
[20]D. G. Mead and J. C. Irwin, Solid State Commun. **20**, 885 (1976).
[21]M. Balkanski, R. F. Wallis, and E. Haro, Phys. Rev. B **28**, 1928 (1983).
[22]P. Verma, S. C. Abbi, and K. P. Jain, Phys. Rev. B **51**, 16660 (1995).
[23]A. Taube, J. Judek, C. Jastrzębski, A. Duzynska, K. Świtkowski, and M. Zdrojek, ACS Appl. Mater. Interfaces **6**, 8959 (2014).
[24]A. Duzynska, J. Judek, and M. Zdrojek, Appl. Phys. Lett. **105**, 213105 (2014).
[25]Z. Yan, C. Jiang, T. R. Pope, C. F. Tsang, J. L. Stickney, P. Goli, J. Renteria, T. T. Salguero, and A. A. Balandin, J. Appl. Phys. **114**, 204301 (2013).
[26]I. Calizo, S. Ghosh, W. Bao, F. Miao, C. N. Lau, and A. A. Balandin, Solid State Commun. **149**, 1132 (2009).
[27]D. J. Late, ACS Appl. Mater. Interfaces **7**, 5857 (2015).
[28]M. Thripuranthaka, R. V. Kashid, C. S. Rout, and D. J. Late, Appl. Phys. Lett. **104**, 081911 (2014).
[29]M. Thripuranthaka and D. J. Late, ACS Appl. Mater. Interfaces **6**, 1158 (2014).
[30]I. Calizo, A. A. Balandin, W. Bao, F. Miao, and C. N. Lau, Nano Lett. **7**, 2645 (2007).
[31]S. Zhang, J. Yang, R. Xu, F. Wang, W. Li, M. Ghufran, Y.-W. Zhang, Z. Yu, G. Zhang, Q. Qin, and Y. Lu, ACS Nano **8**, 9590 (2014).
[32]D. J. Late, S. N. Shirodkar, U. V. Waghmare, V. P. Dravid, and C. N. R. Rao, ChemPhysChem **15**, 1592 (2014).
[33]K. Grodecki, J. A. Blaszczyk, W. Strupinski, A. Wysmolek, R. Stępniewski, A. Drabinska, M. Sochacki, A. Dominiak, and J. M. Baranowski, J. Appl. Phys. **111**, 114307 (2012).
[34]A. A. Balandin, Nat. Mater. **10**, 569 (2011).
[35]A. A. Balandin, S. Ghosh, W. Bao, I. Calizo, D. Teweldebrhan, F. Miao, and C. N. Lau, Nano Lett. **8**, 902 (2008).
[36]A. Taube, J. Judek, A. Łapińska, and M. Zdrojek, ACS Appl. Mater. Interfaces **7**, 5061 (2015).
[37]M. Freitag, M. Steiner, Y. Martin, V. Perebeinos, Z. Chen, J. C. Tsang, and P. Avouris, Nano Lett. **9**, 1883 (2009).
[38]Z. Yan, G. Liu, J. M. Khan, and A. A. Balandin, Nat. Commun. **3**, 827 (2012).